Lower hybrid waves at the magnetosheath separatrix region

Binbin Tang[1*], Wenya Li[1], Daniel Graham[2], Chi Wang[1], Yuri Khotyaintsev[2], Barbara L. Giles[3], Per-Arne Lindqvist[4], Robert E. Ergun[5], Christopher T. Russell[6], and James L. Burch[7]

(* bbtang@spacewether.ac.cn)

[1] National Space Science Center, CAS, China

[2] Swedish Institute of Space Physics, Uppsala, Sweden

[3] NASA Goddard Space Flight Center, Greenbelt, MD, USA

[4] KTH Royal Institute of Technology, Stockholm, Sweden

[5] Laboratory of Atmospheric and Space Physics, University of Colorado Boulder, Boulder, Colorado, USA

[6] Department of Earth and Space Sciences, University of California, Los Angeles, California, USA.

[7] Southwest Research Institute, San Antonio, Texas, USA.

EGU_Online_2020 4 May 2020

Basic properties of lower hybrid waves (LHWs)

- Frequency: $f_{ci} < f < f_{ce}$
- Wavelength: $\rho_i > \lambda > \rho_e$

→ electrons: approximated magnetized

ions: almost unmagnetized

- quasi-electrostatic, but δ**B** are not zero (the ratio W_B/W_E is often >1 at magnetopause)
- $k_\perp >> k_{||}$

→Linearly polarized and δB mainly in parallel directions

- More details can be found at Graham et al., [2019].

Lower hybrid waves (LHWs) at Earth's magnetopause

- LHWs are frequently observed at magnetospheric side of the magnetopause reconnection, which can be generated by

a. Lower hybrid drift instability: a density/temperature gradient

b. Modified two-stream instability: beam-like finite gyroradius ions

- LHWs are of particular importance

a. cross-field particle diffusion → built-up of LLBL

b. anomalous resistivity/ viscosity

c. …

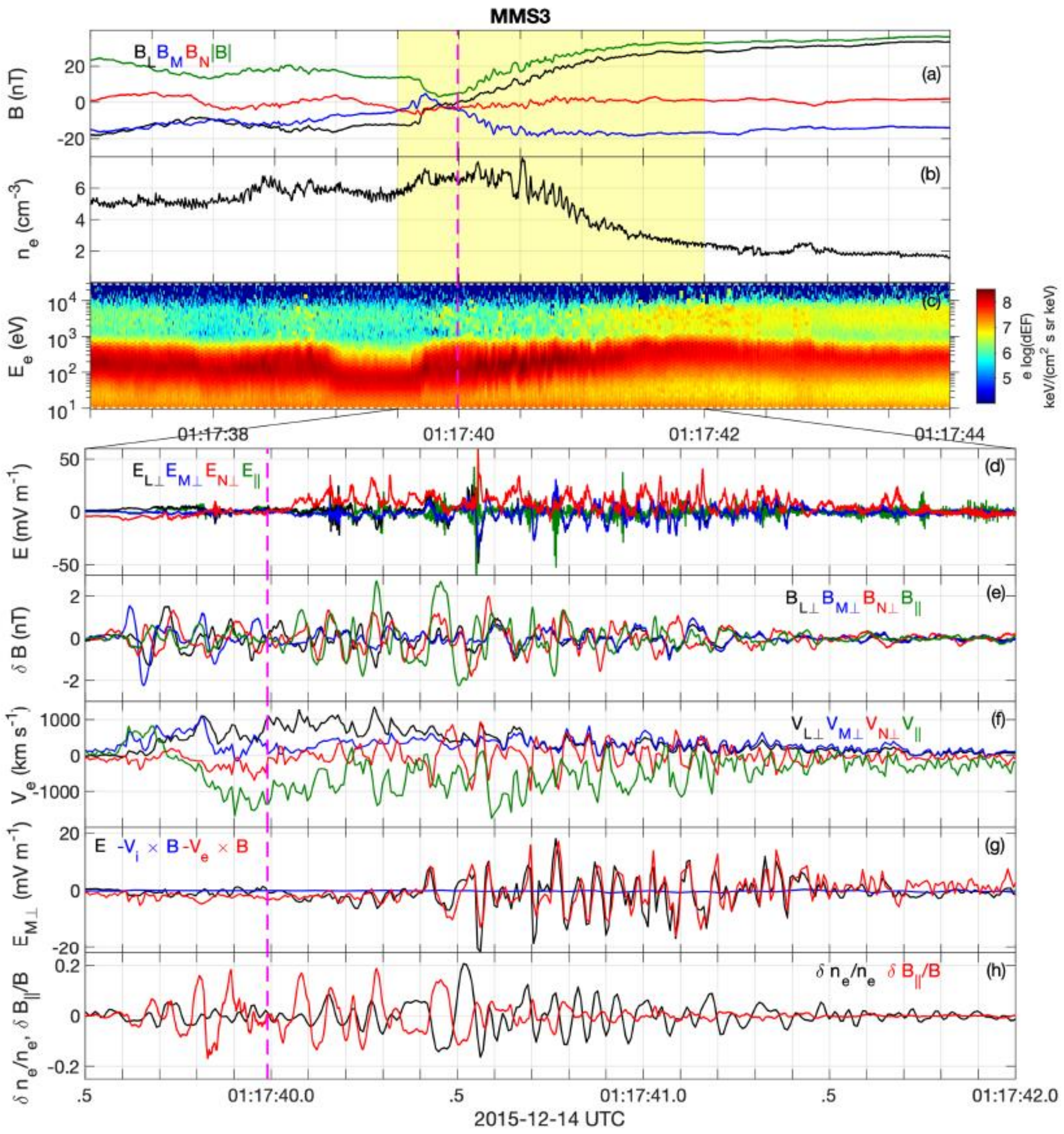

Graham et al., 2019

Asymmetric guide-field reconnection

- Asymmetry of the reconnection exhaust: $B_g \pm B_{Hall}$

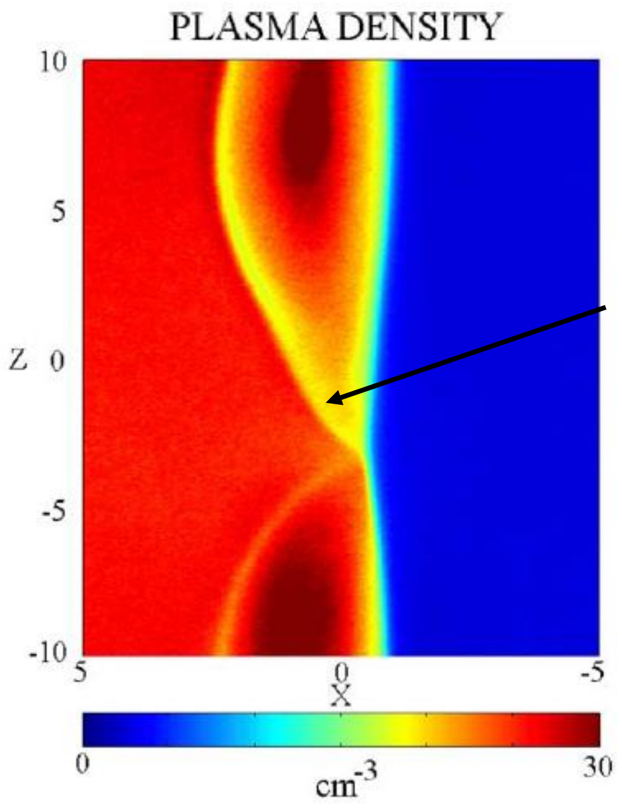

Strong B_M

Density gradient

Weak B_M

Mozer et al., 2008

Clear perturbations of LHWs?

Also some perturbations.
Lower hybrid waves?

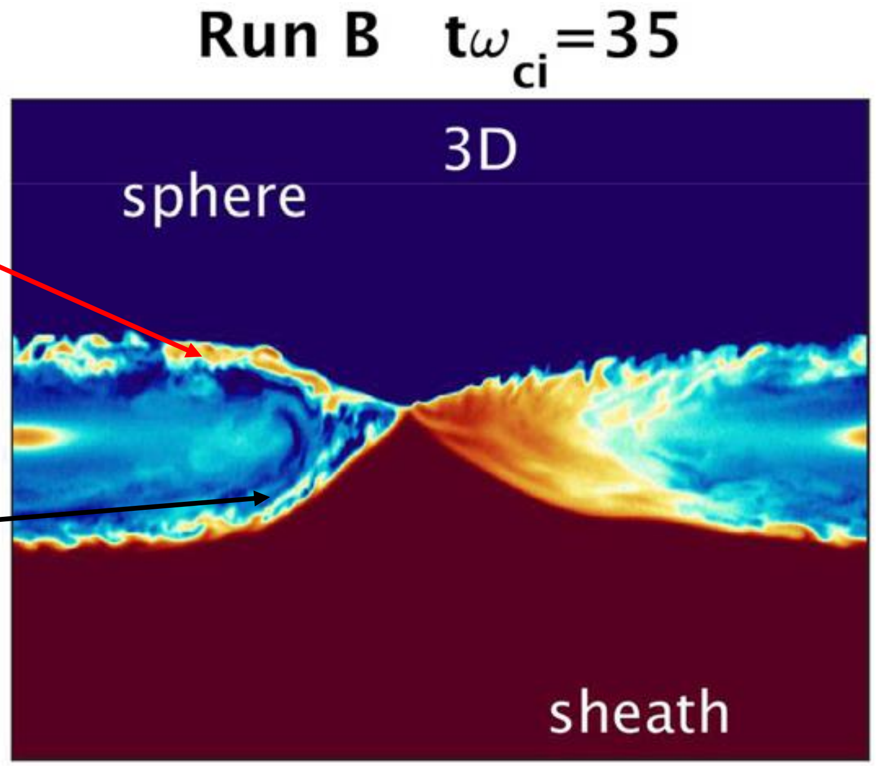

$B_g = 0.4$ Le et al., 2018

Event overview

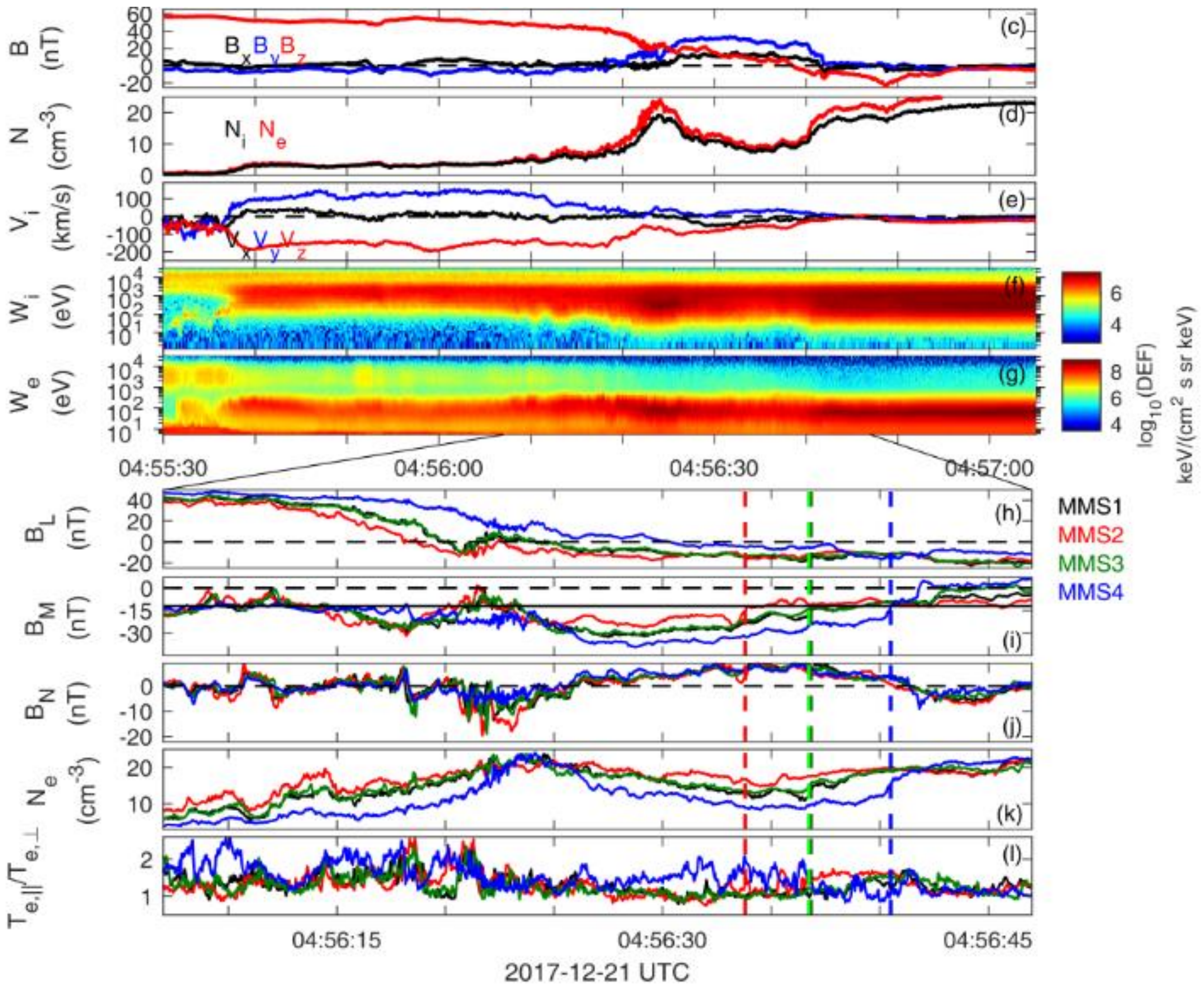

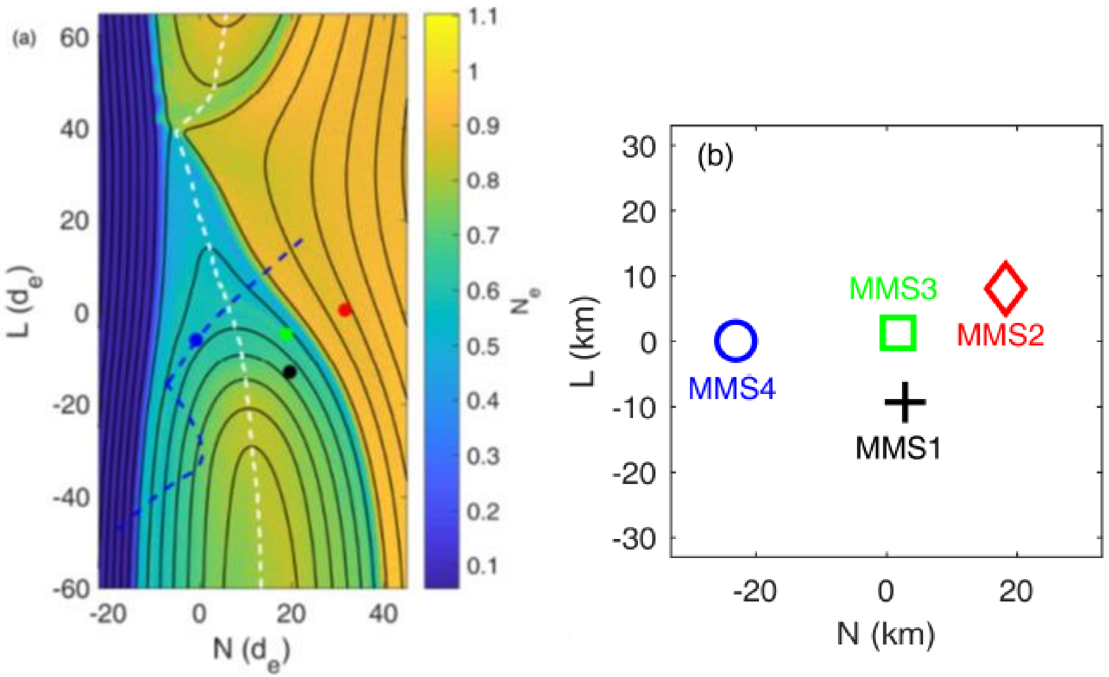

- From the x-line to downstream (due to the large tangential motion)

  MMS 4 → MMS 1, 3 → MMS 2

- Slow normal motion ($V_{mp,N}$ ~ 5 km/s)
- Significant different MMS observations
- Clear density gradient is found at the sheath separatrix (marked by the vertical dashed line)

Zoom-in at the magnetosheath separatrix

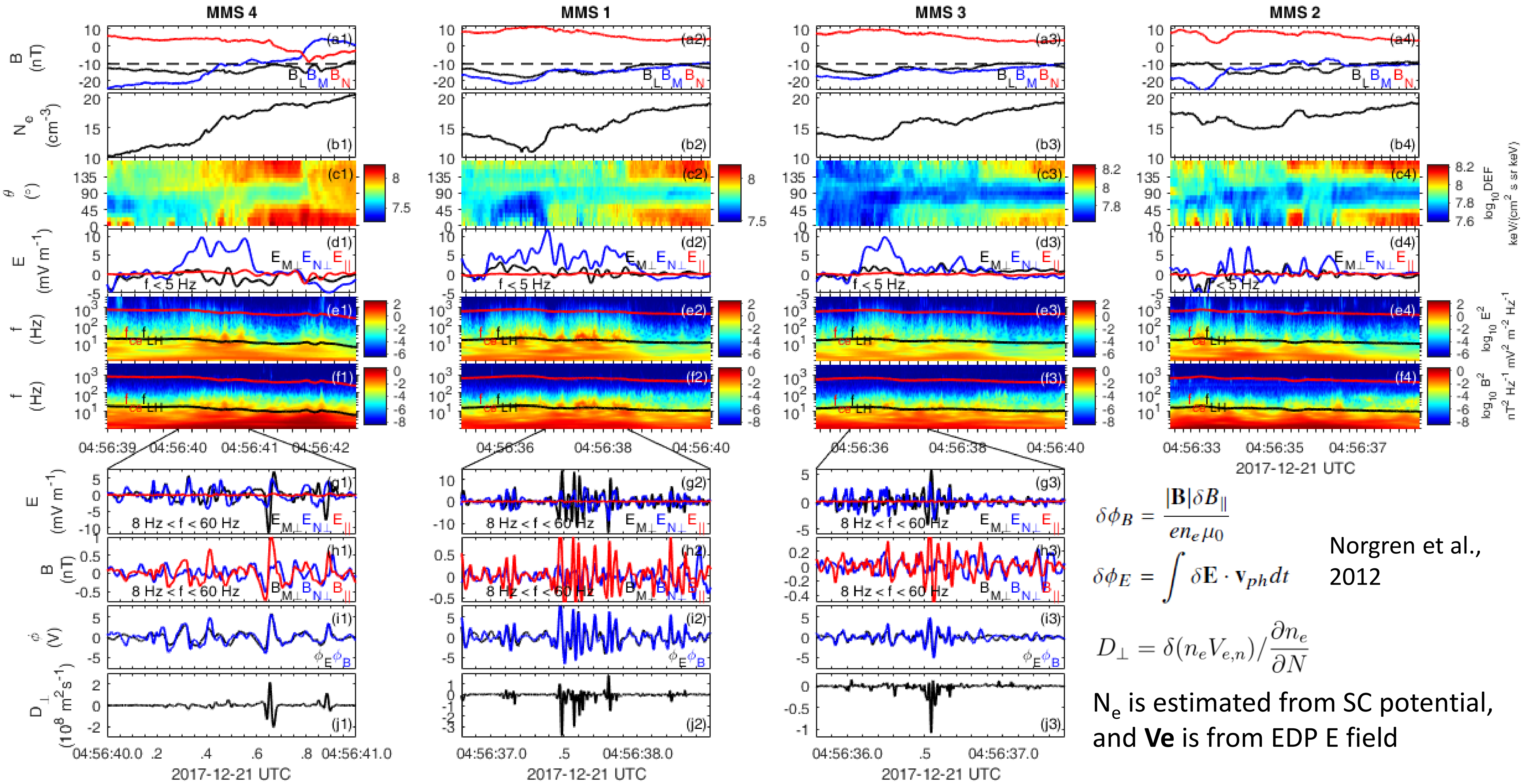

$$\delta\phi_B = \frac{|\mathbf{B}|\delta B_{\parallel}}{e n_e \mu_0}$$

$$\delta\phi_E = \int \delta\mathbf{E}\cdot\mathbf{v}_{ph}dt$$

Norgren et al., 2012

$$D_\perp = \delta(n_e V_{e,n})/\frac{\partial n_e}{\partial N}$$

N_e is estimated from SC potential, and **Ve** is from EDP E field

Properties of observed LHWs

	V_{ph} (km/s)	λ (km)	$k_\perp \rho_e$	Φ_B (V)	Φ_E (V)	C_Φ	$\langle D_\perp \rangle$ ($m^2 s^{-1}$)
MMS4	50 × [0.62 -0.71 -0.33]	4.2	1.0	5.7	5.8	0.83	~ 10^5
MMS1	65 × [0.72 -0.70 0.06]	3.1	1.6	7.8	8.4	0.87	-2.6 × 10^7
MMS3	94 × [0.67 -0.72 -0.18]	6.3	0.9	5.2	4.5	0.81	-1.8 × 10^7

- Due to the presence of the magnetic B_M, the propagation direction of these waves is not closed aligned in -M direction, but has a component in L direction. → For comparison, LHWs at the magnetospheric side propagate approximately in M direction (in the ion rest frame).
- $k_\perp \rho_e \sim 1 – 1.6$
- The sheath electron temperature is about 30 eV, leading to $e\Phi/k_B T_e \sim$ 15% - 25%
- $\langle D_\perp \rangle$ here is 1~2 orders in magnitude smaller than it in the magnetospheric side. Still it will only take several seconds to diffusely transport electrons if assuming the boundary is ~10 km thick.

Properties of observed LHWs

	$\mathbf{k}$ (LMN)	V_{ph} (km/s)	Φ_B (V)	Φ_E (V)	C_Φ	$k_\perp \rho_e$	V_{ph} (km/s)	f (Hz)	$k_\perp \rho_e$	$\langle D_\perp \rangle$ ($m^2 s^{-1}$)
	Norgren et al. [2012]						Graham et al. [2019]			
MMS4	[0.62 -0.71 -0.33]	50	5.7	5.8	0.83	1.0	43	8.6	1.2	$\sim 10^5$
MMS1	[0.72 -0.70 0.06]	65	7.8	8.4	0.87	1.6	53	20.4	2.1	-2.6×10^7
MMS3	[0.67 -0.72 -0.18]	94	5.2	4.5	0.81	0.9	60	17.3	1.4	-1.8×10^7

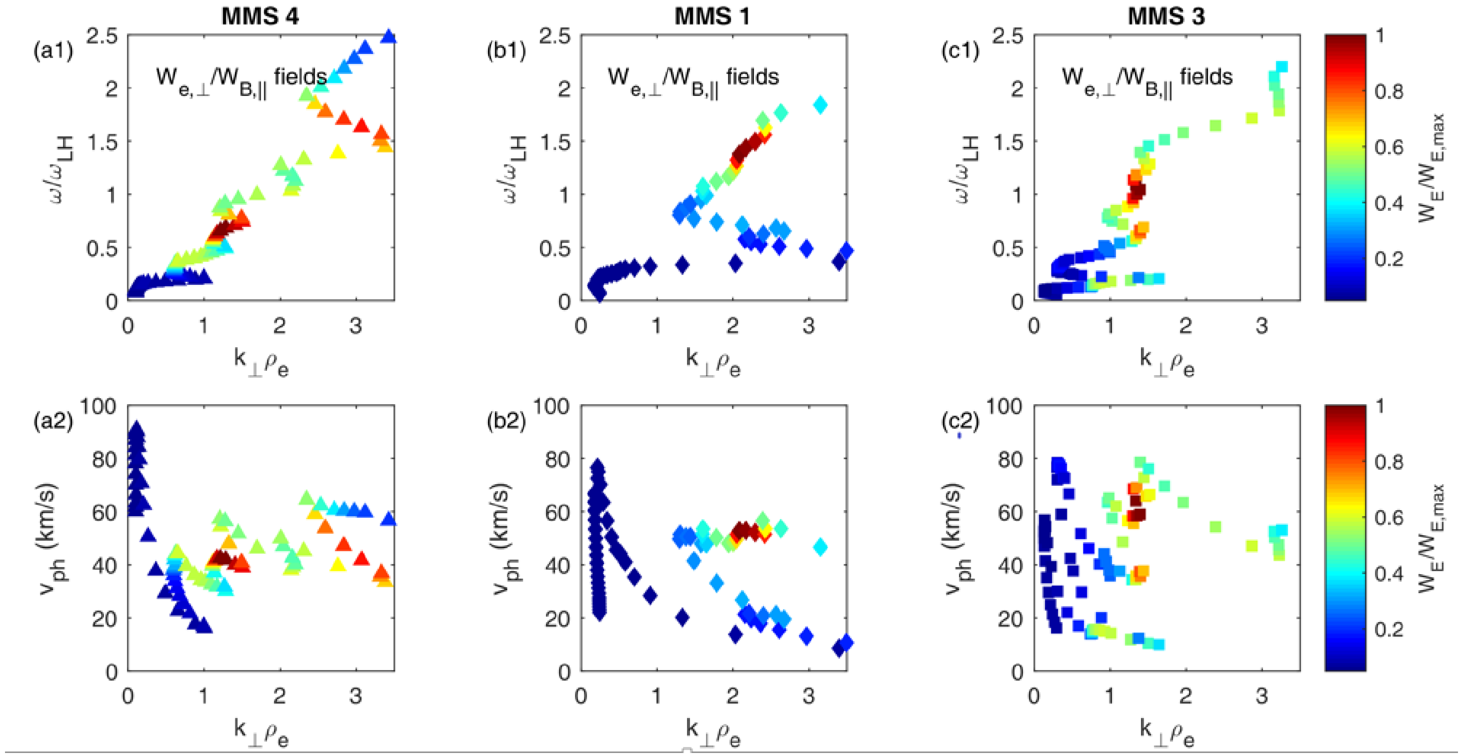

A new method is developed by Graham et al., 2019 to get the wave dispersion relation.

$$k_\perp(\omega) = \frac{1}{d_e}\sqrt{\frac{W_e(\omega)}{W_B(\omega)}},$$

Graham et al., 2019

N_e is estimated from SC potential, and **Ve** is from EDP E field

	k (LMN)	V_{ph} (km/s)	Φ_B (V)	Φ_E (V)	C_Φ	$k_\perp \rho_e$	V_{ph} (km/s)	f (Hz)	$k_\perp \rho_e$	$<D_\perp>$ (m^2s^{-1})
	Norgren et al. [2012]						Graham et al. [2019]			
MMS4	[0.62 -0.71 -0.33]	50	5.7	5.8	0.83	1.0	43	8.6	1.2	~ 10^5
MMS1	[0.72 -0.70 0.06]	65	7.8	8.4	0.87	1.6	53	20.4	2.1	-2.6×10^7
MMS3	[0.67 -0.72 -0.18]	94	5.2	4.5	0.81	0.9	60	17.3	1.4	-1.8×10^7

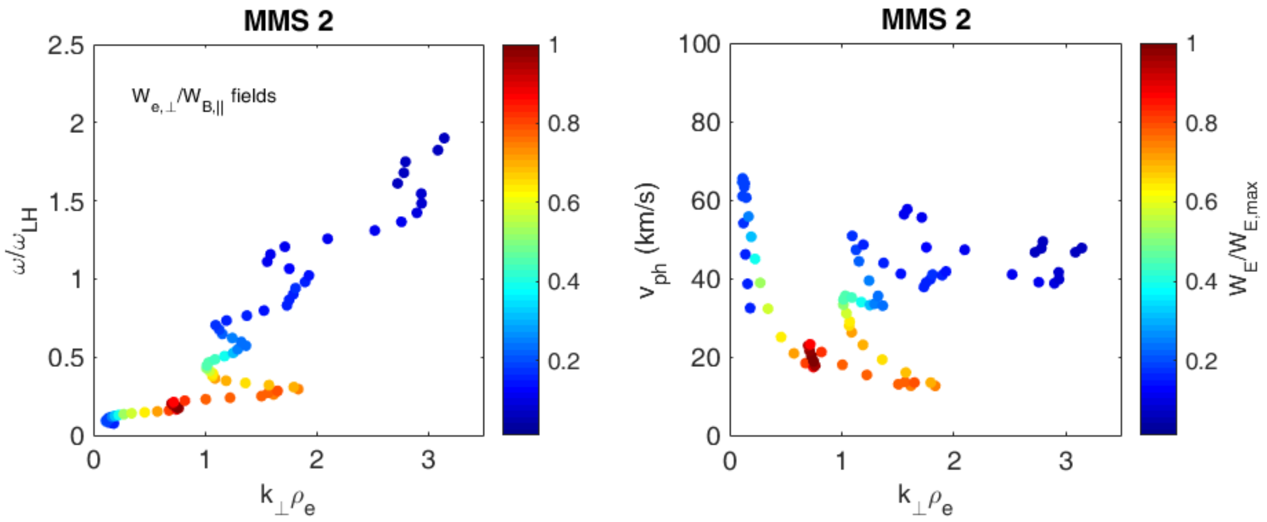

In general, the result from different methods are consistent, but the V_{ph} estimated from Daniel's method seems smaller ($k_\perp$ is larger).

Again, no clear LHWs at MMS 2

Instability analysis (a finite plasma beta, ion frame)

$$0 = 1 - \frac{\omega_{pi}^2}{k^2 v_i^2} Z'\left(\frac{\omega}{k v_i}\right) + \frac{\omega_{pe}^2}{\Omega_{ce}^2}\left(1 + \frac{\omega_{pe}^2}{c^2 k^2}\right) + \frac{2\omega_{pe}^2}{k^2 v_e^2}\left(1 + \frac{\beta_i}{2}\right)\frac{k V_{de}}{\omega - k V_E},$$

$$\mathbf{V}_{e\perp} \approx \mathbf{V}_E + \mathbf{V}_{de}$$

Davidson et al., 1977

	k (LMN)	V_{ph} (km/s)	Φ_B (V)	Φ_E (V)	C_Φ	$k_\perp \rho_e$	V_{ph} (km/s)	f (Hz)	$k_\perp \rho_e$	$\langle D_\perp \rangle$ ($m^2 s^{-1}$)
	Norgren et al. [2012]						Graham et al. [2019]			
MMS4	[0.62 -0.71 -0.33]	50(58)	5.7	5.8	0.83	1.0	43(51)	8.6(9.8)	1.2	$\sim 10^5$
MMS1	[0.72 -0.70 0.06]	65(67)	7.8	8.4	0.87	1.6	53(55)	20.4(20.9)	2.1	-2.6×10^7
MMS3	[0.67 -0.72 -0.18]	94(87)	5.2	4.5	0.81	0.9	60(53)	17.3(15.7)	1.4	-1.8×10^7

The numbers outside/inside the parentheses are estimated in the spacecraft/ion frame.

Instability analysis

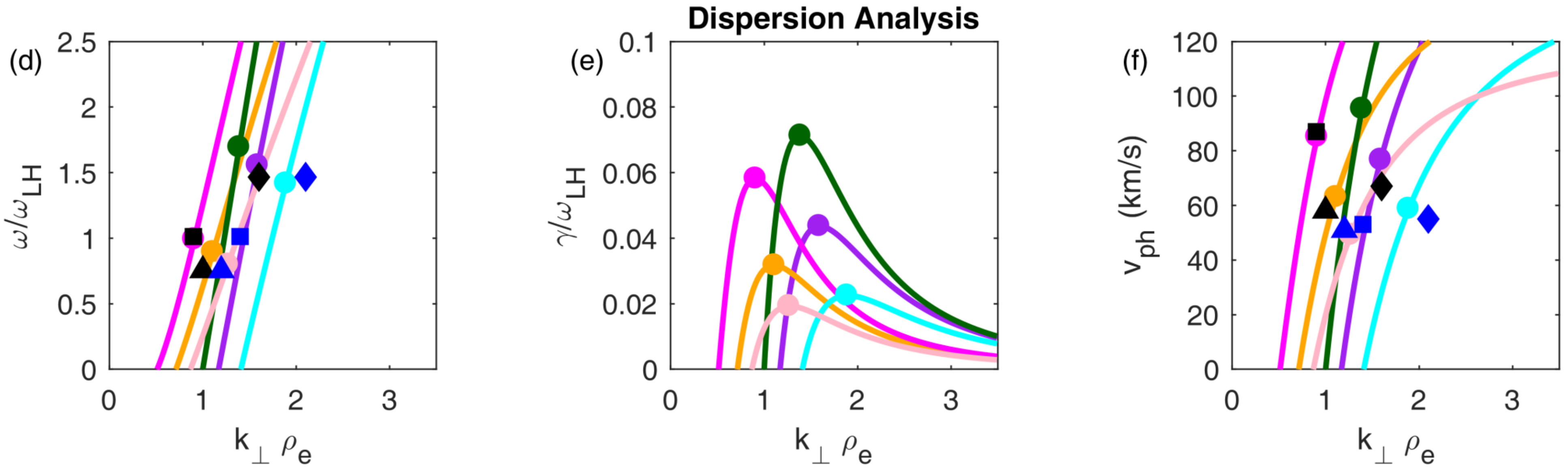

	V_E	V_{de} (km/s)
Pink	120	20
Orange	150	20
Magenta	200	20
Cyan	150	50
Purple	200	50
Green	250	50

Density: 10 cm^{-3}
|B|: 22 nT
β_i: 5.4

Black symbols: Norgren et al. [2012] Blue ones: Graham et al. [2019]

	k (LMN)	V_{ph} (km/s)	Φ_B (V)	Φ_E (V)	C_Φ	$k_\perp \rho_e$	V_{ph} (km/s)	f (Hz)	$k_\perp \rho_e$	$\langle D_\perp \rangle$ ($m^2 s^{-1}$)
	Norgren et al. [2012]						Graham et al. [2019]			
MMS4	[0.62 -0.71 -0.33]	50(58)	5.7	5.8	0.83	1.0	43(51)	8.6(9.8)	1.2	~ 10^5
MMS1	[0.72 -0.70 0.06]	65(67)	7.8	8.4	0.87	1.6	53(55)	20.4(20.9)	2.1	-2.6×10^7
MMS3	[0.67 -0.72 -0.18]	94(87)	5.2	4.5	0.81	0.9	60(53)	17.3(15.7)	1.4	-1.8×10^7

Summary

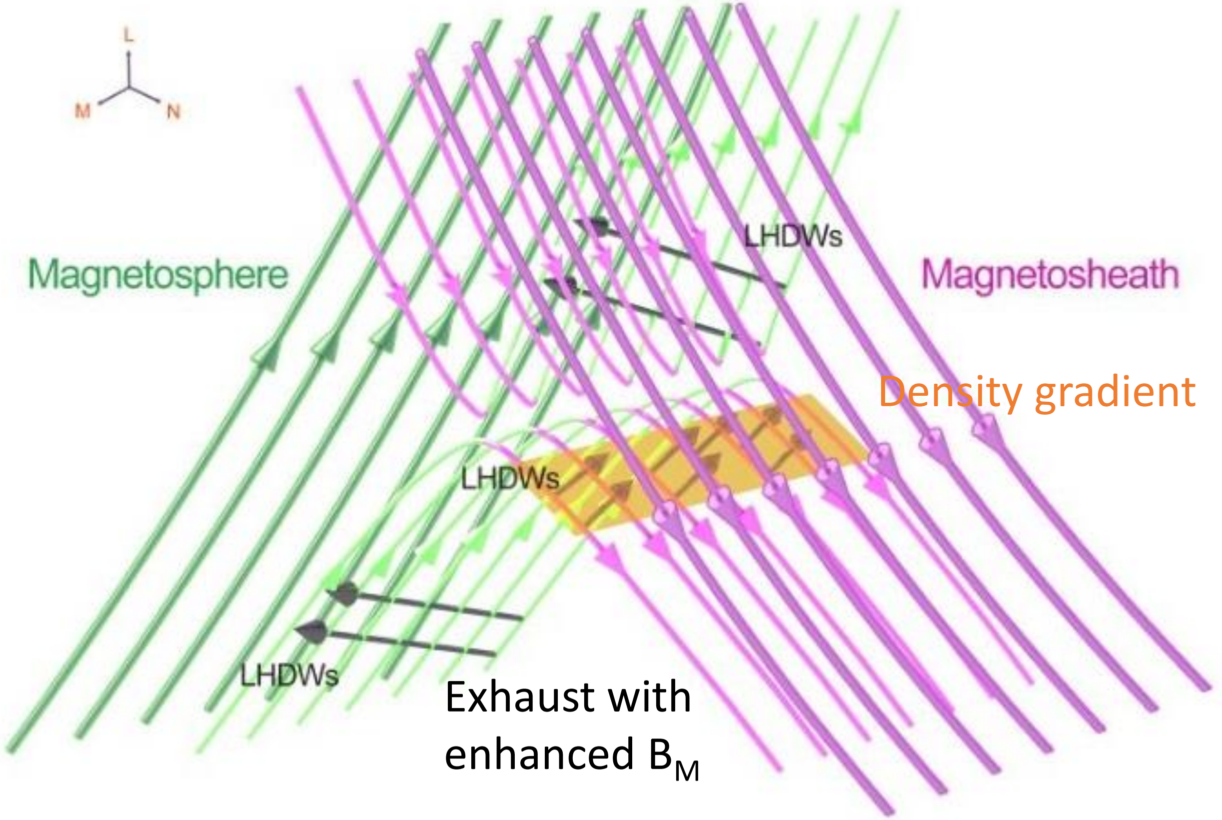

- LHWs are observed at the magnetosheath separatrix in asymmetric guide-field reconnection;
- LHWs are generated by lower hybrid drift instability;
- Properties of these LHWs:
  - ➢ Active in limited regions;
  - ➢ Propagating toward the x-line, in the same direction the diamagnetic drift of the x-line;
  - ➢ $e\Phi/k_BT_e$ ~ 15% - 25% → effectively transport particles from the sheath to the exhaust.

Thank you!

If you have any comments/suggestions, please contact
bbtang@spaceweather.ac.cn